AMERICAN SOCIETY FOR MICROBIOLOGY | Antimicrobial Agents and Chemotherapy®

PHARMACOLOGY

Antiretroviral Penetration across Three Preclinical Animal Models and Humans in Eight Putative HIV Viral Reservoirs

Aaron S. Devanathan,[a] Jason R. Pirone,[a]* Ramesh Akkina,[b] Leila Remling-Mulder,[b] Paul Luciw,[c] Lourdes Adamson,[c] J. Victor Garcia,[d] Martina Kovarova,[d] Nicole R. White,[a] Amanda P. Schauer,[a] Kimberly Blake,[a]* Craig Sykes,[a] Erin M. Burgunder,[a] Nithya Srinivas,[a]* Elias P. Rosen,[a] Angela D. M. Kashuba[a,d]

[a]University of North Carolina Eshelman School of Pharmacy, Chapel Hill, North Carolina, USA
[b]Colorado State University, Fort Collins, Colorado, USA
[c]University of California, Davis, Davis, California, USA
[d]University of North Carolina School of Medicine, Chapel Hill, North Carolina, USA

ABSTRACT For HIV cure strategies like "kick and kill" to succeed, antiretroviral (ARV) drugs must reach effective concentrations in putative viral reservoirs. We characterize penetration of six ARVs in three preclinical animal models and humans. We found that standard dosing strategies in preclinical species closely mimicked tissue concentrations in humans for some, but not all, ARVs. These results have implications for interpreting HIV treatment, prevention, or cure interventions between preclinical and clinical models.

KEYWORDS HIV, antiretrovirals, pharmacokinetics, species differences, tissue reservoirs

Despite 3 decades of improvements in antiretroviral (ARV) therapy, HIV eradication remains elusive. It has been postulated that inadequate ARV penetration into tissues may create pharmacological sanctuaries where HIV continues to replicate (1, 2). For instance, in lymphoid tissues, Fletcher et al. (1) suggested that ARVs do not achieve suppressive concentrations. In cerebrospinal fluid, although the ARV efavirenz (EFV) achieves concentrations at 0.5% of plasma concentrations, this still exceeds the 50% inhibitory concentration for wild-type HIV (3). Because of these tissue penetration and activity differences, a comprehensive analysis is warranted. Because some tissues are impractical to sample from humans, animal models are commonly used in HIV investigations, with standard ARV dosing strategies selected to match human blood plasma exposure. Here, we describe the tissue penetration of six ARVs in two humanized mouse models (hu-HSC [also called RAG-hu in the literature] and bone marrow-liver-thymus [BLT]), nonhuman primates (NHPs), and HIV$^+$ humans. The hu-HSC mice are engrafted with hu-HSC, whereas BLT mice are engrafted with HSC and thymus (4).

The hu-HSC and BLT mice and NHPs were administered standard ARV doses and combinations taken from previously published treatment regimens, and this is summarized in Fig. S1 in the supplemental material (5–12). Tissues harvested from HIV$^+$ patients an estimated 8 to 47 h postdose were obtained from the National NeuroAIDS Tissue Consortium, National Neurological AIDS Bank, and National Research Disease Interchange. Human female genital tract (FGT) and colorectal concentrations were obtained from a clinical trial (NCT01330199). Eight tissue types were examined: brain (median combined concentration of frontal cortex, cerebellum, basal ganglia, and parietal cortex), lymph node (median combined concentration of axillary, iliac, inguinal, and mesenteric lymph nodes), spleen, ileum, rectum, testes, and FGT (median combined concentration of cervix and vagina).

Tissue and plasma concentrations were quantified for (i) the administered ARVs

Citation Devanathan AS, Pirone JR, Akkina R, Remling-Mulder L, Luciw P, Adamson L, Garcia JV, Kovarova M, White NR, Schauer AP, Blake K, Sykes C, Burgunder EM, Srinivas N, Rosen EP, Kashuba ADM. 2020. Antiretroviral penetration across three preclinical animal models and humans in eight putative HIV viral reservoirs. Antimicrob Agents Chemother 64:e01639-19. https://doi.org/10.1128/AAC.01639-19.

Address correspondence to Angela D. M. Kashuba, akashuba@unc.edu.

* Present address: Jason R. Pirone, Nuventra Pharma Sciences, Durham, North Carolina, USA; Kimberly Blake, North Carolina Department of Health and Human Services, Raleigh, North Carolina, USA; Nithya Srinivas, Incyte Corporation, Wilmington, Delaware, USA.

Received 26 August 2019
Returned for modification 19 September 2019
Accepted 8 October 2019
Accepted manuscript posted online 14 October 2019
Published 20 December 2019

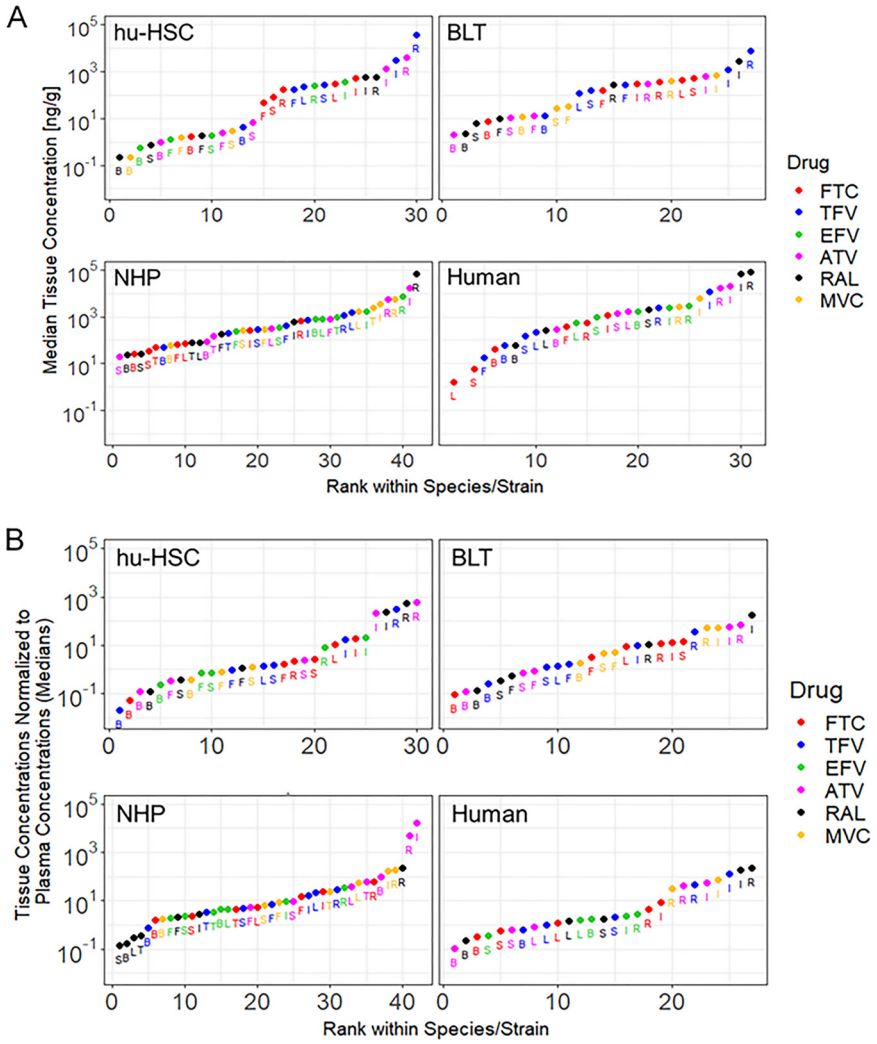

FIG 1 Rank plots of median tissue concentrations (A) and median ratios of tissue-to-plasma concentrations (B). Antiretroviral abbreviations: ATV, atazanavir; EFV, efavirenz; FTC, emtricitabine; MVC, maraviroc; RAL, raltegravir; TFV, tenofovir. Tissue abbreviations: B, brain; F, female genital tract; I, ileum; L, lymph node; R, rectum; S, spleen; T, testes. NHP, nonhuman primate. BLT mice were not dosed with EFV due to toxicity concerns. Testes were only evaluated in NHPs.

emtricitabine (FTC), tenofovir (TFV), EFV, raltegravir (RAL), maraviroc (MVC), and atazanavir (ATV) (5–7, 10); (ii) the two active metabolites tenofovir diphosphate (TFVdp) and emtricitabine triphosphate (FTCtp) (13); and (iii) two endogenous nucleotides (dATP and dCTP). Concentrations were converted from nanogram per milliliter to nanogram per gram using a tissue density of 1.06 g/ml. Where measurements of ARV concentrations were below the limit of quantification, we imputed a value of one-half of the lower limit of quantification. Metabolite-to-endogenous nucleotide ratios (active metabolite/tissue endogenous nucleotide concentration) for each tissue were analyzed via the Wilcoxon rank-sum test with the Benjamini Hochberg *P* value adjustment procedure. Spearman's rank correlation coefficients were calculated to illustrate the relationships between plasma and tissue concentrations. All analyses were performed using R 3.5.3 (Vienna, Austria).

Comparisons of ARV concentrations across multiple tissues and multiple species are shown in a rank plot in Fig. 1A, where data are grouped by species/model. Median tissue concentrations were ranked from lowest to highest. For all species and ARVs, concentrations were highest in the gastrointestinal tract (GIT; either ileum or rectum). In tissues where exposure to an ARV could be compared in at least two different

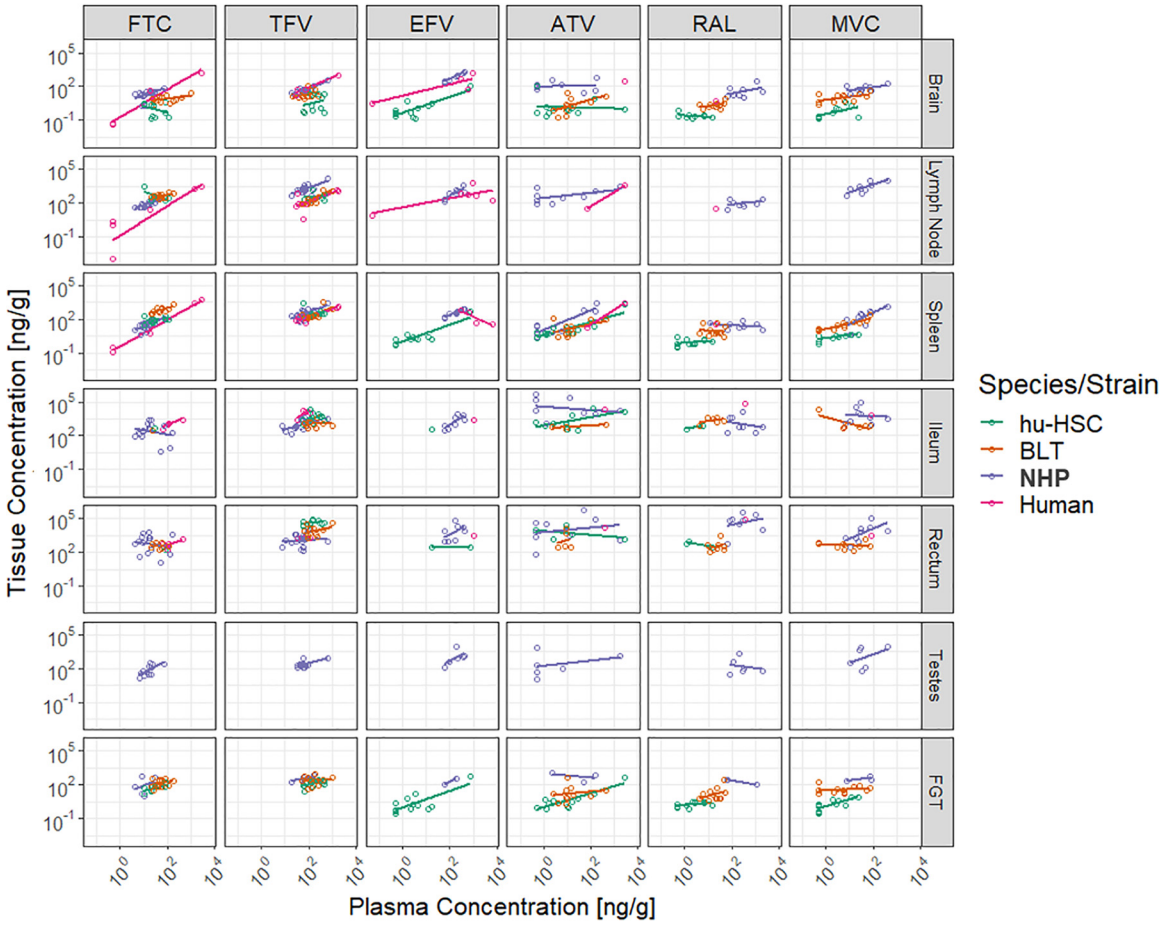

FIG 2 Correlation plots of tissue versus plasma concentrations across all tissues for the six antiretrovirals. Antiretroviral abbreviations: ATV, atazanavir; EFV, efavirenz; FTC, emtricitabine; MVC, maraviroc; RAL, raltegravir; TFV, tenofovir. FGT, female genital tract; NHP, nonhuman primate. BLT mice were not dosed with EFV due to toxicity concerns. Testes were only evaluated in NHPs.

species, the lowest ARV concentrations were observed mostly in hu-HSCs (18 out of 36 paired tissue-ARV measurements). Notable exceptions were found in lymph node, spleen, and FGT, where the lowest concentrations for the nucleoside reverse transcriptase inhibitors (NRTIs) FTC and TFV were measured in humans. When normalizing to plasma, the trends seen in each species for the tissue concentration rank plot were seen in the normalized-concentrations rank plot (Fig. 1B).

Correlation plots of ARV concentrations in tissue versus plasma were used to evaluate the proclivity of ARVs to penetrate into tissues and are shown in Fig. 2, and individual Spearman's rank correlation coefficients are shown in Table 1. These plots and coefficients illustrate two things. First, generally, as plasma concentrations increased, the tissue concentrations increased. Across most species, the plots suggested that increasing the NRTI dose would result in increased tissue penetration in lymph node and spleen. This was confirmed numerically by the correlation coefficients. Second, less-clear trends were seen in ATV correlation plots, which indicated insignificant correlations (increased plasma concentrations did not correlate with increased tissue concentrations) consistently for NHPs and RAL correlation plots, which were inconsistent among species but were generally negative in NHPs and hu-HSC mice.

Because the efficacy of the active NRTI metabolite competes with the endogenous nucleotide it replaces during the reverse transcription process (14), we calculated the ratios of intracellular active metabolite to endogenous nucleotide concentrations against 90% effective concentration cutoffs derived from $CD4^+$ T cells by Cottrell et al. (13). As seen in Fig. 3, FTCtp/dCTP ratios in mouse models in the lymphoid organs were

TABLE 1 Correlation coefficients of plasma and tissue concentrations for 6 antiretrovirals

	Antiretrovirals and correlation coefficients[b]					
Tissue[a]	FTC	TFV	EFV	ATV	RAL	MVC
Brain						
hu-HSC	−0.3	0.2	0.5	0.1	−0.1	0.5
BLT	0.3	0.3	—	0.6[c]	0.4	0.5
NHP	0.7[c]	0.7[c]	0.98[c]	0.1	0.2	0.3
Human	0.9	0.8	0.8	N1	N1	—
Lymph node						
hu-HSC	−0.5	0.3	BLQ	BLQ	BLQ	BLQ
BLT	0.2	0.7[c]	—	BLQ	BLQ	BLQ
NHP	0.9[c]	0.6[c]	0.8[c]	0.5	0.3	0.7
Human	0.9[c]	0.5	0.03	1.0	N1	—
Spleen						
hu-HSC	0.5	0.4	0.4	0.7[c]	0.4	0.5
BLT	0.6	0.6	—	0.3	0.06	0.9[c]
NHP	0.8[c]	0.6[c]	0.9[c]	0.7	−0.2	0.8[c]
Human	0.91[c]	0.6	−1.0	1.0	N1	—
Ileum						
hu-HSC	N1	0.5[c]	N1	0.4	1.0	BLQ
BLT	N1	0.1	—	0.7	0.1	0.1
NHP	0.2	0.5[c]	0.8[c]	−0.4	−0.1	−0.1
Human	1.0	0.2	N1	N1	N1	N1
Rectum						
hu-HSC	N1	0.4	−1.0	−0.5	−0.5	BLQ
BLT	−0.1	0.1	—	−0.1	0.2	−0.3
NHP	−0.1	0.2	0.6	0.2	0.4	0.8[c]
Human	0.8	−0.4	N1	N1	N1	N1
Testes						
hu-HSC	—	—	—	—	—	—
BLT	—	—	—	—	—	—
NHP	0.6[c]	0.1	0.7	0.3	0.1	0.1
Human	—	—	—	—	—	—
FGT						
hu-HSC	0.7[c]	0.5	0.6	0.7[c]	0.5	0.8[c]
BLT	0.3	−0.04	—	0.4	0.3	0.2
NHP	0.1	0.6	1.0	−0.5	−1.0	0.5
Human	—	—	—	—	—	—

[a]BLT mice were not dosed with EFV due to toxicity concerns. Testes were only evaluated in NHPs. FGT, female genital tract.

[b]ATV, atazanavir; EFV, efavirenz; FTC, emtricitabine; MVC, maraviroc; RAL, raltegravir; TFV, tenofovir; —, tissues not evaluated; N1, correlation coefficient not evaluable due to only one pair of plasma and tissue concentrations; BLQ, below the limit of quantification.

[c]$P < 0.05$ via Spearman's rank correlation.

not significantly different from those in humans. TFVdp/dATP ratios were similar in mouse models and humans except for spleen and FGT. Ratios in NHPs were similar to, or higher than, those in humans. In lymph node, spleen, and FGT, TFVdp/dATP ratios were significantly higher (up to 161-fold) in NHPs than in humans, despite similar plasma concentrations between the two species; in the rectum, 1.9- to 105-fold-higher ratios were noted in NHPs than in humans for both NRTIs.

To our knowledge, this is the first analysis of ARV tissue penetration across multiple HIV putative reservoirs in multiple species using standard dosing strategies (8, 10, 12). Based on the correlation plots and coefficient values, we found that current ARV doses in NHPs mimic human plasma and tissue exposure, whereas mice generally have lower and more inconsistent penetration across tissues. This suggests similar tissue penetration processes for most ARVs between NHPs and humans. Our results have several important implications. First, we have shown significant heterogeneity in ARV pene-

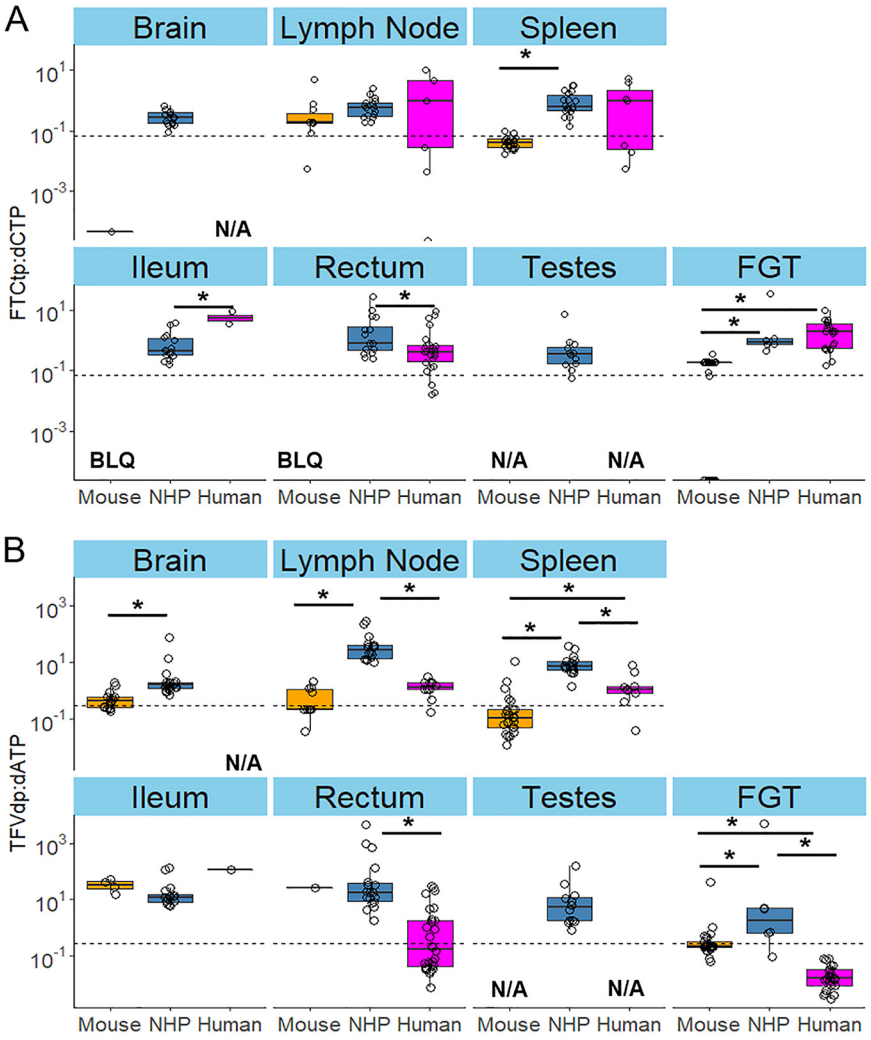

FIG 3 Metabolite-to-endogenous nucleotide ratio boxplots across eight tissues for FTCtp (A) and TFVdp (B). Dotted lines represent literature-derived 90% effective concentrations. NHP, nonhuman primate; BLQ, below limit of quantification; N/A, not applicable; FGT, female genital tract; FTCtp, emtricitabine triphosphate; TFVdp, tenofovir diphosphate. Testes were only evaluated in NHPs. *, $P < 0.05$ via Wilcoxon rank-sum test with Benjamini Hochberg *P* value adjustment procedure.

tration between tissues (e.g., concentrations across species in lymph nodes were 7-fold lower than in the rectum), underscoring crucial pharmacological differences between tissues. Second, we noted heterogeneity between species (e.g., TFVdp concentrations were higher in NHP FGT and mouse and NHP rectums than in the respective human tissues, despite TFV concentrations in NHPs being ~2-fold higher than in mouse models) with standard dosing protocols. This suggests that TFV concentrations may overpredict efficacy in mice and NHPs versus humans. Third, we noted that inconsistent relationships between plasma and tissue concentrations exist with RAL, whereas a positive linear relationship exists for NRTIs in the secondary lymphoid organs, which underlines not only the heterogeneity of ARV penetration among tissues but also the importance of the secondary lymphoid organs as reservoirs (15, 16). Fourth, we noted that NHPs achieve higher metabolite/nucleotide ratios than mouse models and humans in the secondary lymphoid organs and in the FGT, and the ratios for NHPs are higher than those seen in humans in the GIT. Taken together, we discovered important differences that should be considered when translating from preclinical species to humans.

Biochemical and physiological differences related to absorption and elimination

between preclinical models and humans can result in additional variability in plasma concentrations and, consequently, tissue concentrations (17, 18). Figures 2 and 3 represent tissue concentrations normalized to accompanying plasma concentrations, thereby providing a visualization of penetration into respective tissues by species at one point in time.

The current analysis has several limitations. Liquid chromatography-tandem mass spectrometry analysis of tissue homogenates provides an average concentration within tissues. We previously reported that spatial information can be gleaned from infrared matrix-assisted laser desorption electrospray ionization imaging analyses of sanctuary site tissue slices (6, 19–21). This work is ongoing. This analysis also focused on total-drug concentrations rather than protein-unbound concentrations, although NRTIs demonstrate low protein binding potential. Because the unbound ARV concentrations are responsible for pharmacological effects, it is important to compare these differences in the future. As of this writing, the tissue protein binding potential for EFV, RAL, MVC, and ATV has been measured in the brain of NHPs (6), suggesting lower protein binding in tissues than in plasma in all species.

Because ARVs are substrates for drug transporters, particularly the solute carrier and ATP-binding cassette transporter superfamilies, their tissue concentrations may be modulated by transporter activity (22). Although the current analysis did not examine the influence of drug transporters, our group has found that transporter RNA or protein tissue concentrations alone do not accurately correlate with ARV concentrations in gut-associated lymphoid tissue (5) and lymph node (7). Physicochemical properties of ARVs, such as lipophilicity and pH trapping, may contribute to tissue drug concentration. For instance, EFV has a log *P* value of 4.6, which is favorable for tissue distribution (23). Log *P*, pK_a, and percent protein binding values and drug transporter affinities of the analyzed ARVs are displayed in Table S1 in the supplemental material.

In conclusion, drug concentrations in different tissues vary among different species. Whereas data in NHPs agree with some data in humans, humanized mouse models are in concordance with other data in humans, depending on the tissues and individual drugs evaluated. These results suggest that drug exposure in tissues should be evaluated in preclinical models when considering scaling interventions to humans and that increased plasma concentrations do not always translate to tissue penetration, an important finding in view of proposed intensification strategies.

SUPPLEMENTAL MATERIAL

Supplemental material is available online only.

SUPPLEMENTAL FILE 1, PDF file, 0.1 MB.

ACKNOWLEDGMENTS

This work was supported by the following funding sources: NIH R01AI111891 (to A.D.M.K.), NIH P30AI50410 (University of North Carolina at Chapel Hill Center for AIDS Research), NIH U01AI095031 (to A.D.M.K.), and P51OD011107 (California National Primate Research Center). This work was supported by shared resources through NIMH and NINDS by the following grants: U24MH100931 (Manhattan HIV Brain Bank), U24MH100930 (Texas Neuro AIDS Research Center), U24MH100929 (National Neurological AIDS Bank), and U24MH100928 (California NeuroAIDS Tissue Network).

A.S.D. is supported by the National Institute of General Medical Sciences, NIH, under award number T32GM086330.

We thank Howard Fox and Elizabeth Kulka of the National NeuroAIDS Tissue Consortium for providing the human tissue samples for brain, lymph node, and spleen in this study.

The content is solely the responsibility of the authors and does not necessarily represent the official views of the National Institutes of Health.

REFERENCES

1. Fletcher CV, Staskus K, Wietgrefe SW, Rothenberger M, Reilly C, Chipman JG, Beilman GJ, Khoruts A, Thorkelson A, Schmidt TE, Anderson J, Perkey K, Stevenson M, Perelson AS, Douek DC, Haase AT, Schacker TW. 2014. Persistent HIV-1 replication is associated with lower antiretroviral drug concentrations in lymphatic tissues. Proc Natl Acad Sci U S A 111:2307–2312. https://doi.org/10.1073/pnas.1318249111.
2. Huang Y, Hoque MT, Jenabian M-A, Vyboh K, Whyte S-K, Sheehan NL, Brassard P, Bélanger M, Chomont N, Fletcher CV, Routy J-P, Bendayan R. 2016. Antiretroviral drug transporters and metabolic enzymes in human testicular tissue: potential contribution to HIV-1 sanctuary site. J Antimicrob Chemother 71:1954–1965. https://doi.org/10.1093/jac/dkw046.
3. Best BM, Koopmans PP, Letendre SL, Capparelli EV, Rossi SS, Clifford DB, Collier AC, Gelman BB, Mbeo G, McCutchan JA, Simpson DM, Haubrich R, Ellis R, Grant I, CHARTER Group. 2011. Efavirenz concentrations in CSF exceed IC50 for wild-type HIV. J Antimicrob Chemother 66:354–357. https://doi.org/10.1093/jac/dkq434.
4. Akkina R. 2013. New generation humanized mice for virus research: comparative aspects and future prospects. Virology 435:14–28. https://doi.org/10.1016/j.virol.2012.10.007.
5. Thompson CG, Fallon JK, Mathews M, Charlins P, Remling-Mulder L, Kovarova M, Adamson L, Srinivas N, Schauer A, Sykes C, Luciw P, Garcia JV, Akkina R, Smith PC, Kashuba A. 2017. Multimodal analysis of drug transporter expression in gastrointestinal tissue. AIDS 31:1669–1678. https://doi.org/10.1097/QAD.0000000000001554.
6. Srinivas N, Rosen EP, Gilliland WM, Kovarova M, Remling-Mulder L, De La Cruz G, White N, Adamson L, Schauer AP, Sykes C, Luciw P, Garcia JV, Akkina R, Kashuba A. 2019. Antiretroviral concentrations and surrogate measures of efficacy in the brain tissue and CSF of preclinical species. Xenobiotica 49:1192–1201. https://doi.org/10.1080/00498254.2018.1539278.
7. Burgunder E, Fallon JK, White N, Schauer AP, Sykes C, Remling-Mulder L, Kovarova M, Adamson L, Luciw P, Garcia JV, Akkina R, Smith PC, Kashuba A. 2019. Antiretroviral drug concentrations in lymph nodes: a cross-species comparison of the effect of drug transporter expression, viral infection, and sex in humanized mice, nonhuman primates, and humans. J Pharmacol Exp Ther 370:360–368. https://doi.org/10.1124/jpet.119.259150.
8. Denton PW, Krisko JF, Powell DA, Mathias M, Kwak YT, Martinez-Torres F, Zou W, Payne DA, Estes JD, Garcia JV. 2010. Systemic administration of antiretrovirals prior to exposure prevents rectal and intravenous HIV-1 transmission in humanized BLT mice. PLoS One 5:e8829. https://doi.org/10.1371/journal.pone.0008829.
9. Neff CP, Ndolo T, Tandon A, Habu Y, Akkina R. 2010. Oral pre-exposure prophylaxis by anti-retrovirals raltegravir and maraviroc protects against HIV-1 vaginal transmission in a humanized mouse model. PLoS One 5:e15257. https://doi.org/10.1371/journal.pone.0015257.
10. Veselinovic M, Yang K-H, LeCureux J, Sykes C, Remling-Mulder L, Kashuba ADM, Akkina R. 2014. HIV pre-exposure prophylaxis: mucosal tissue drug distribution of RT inhibitor tenofovir and entry inhibitor maraviroc in a humanized mouse model. Virology 464–465:253–263. https://doi.org/10.1016/j.virol.2014.07.008.
11. Massud I, Martin A, Dinh C, Mitchell J, Jenkins L, Heneine W, Pau C-P, García-Lerma JG. 2015. Pharmacokinetic profile of raltegravir, elvitegravir and dolutegravir in plasma and mucosal secretions in rhesus macaques. J Antimicrob Chemother 70:1473–1481. https://doi.org/10.1093/jac/dku556.
12. Shytaj IL, Norelli S, Chirullo B, Della Corte A, Collins M, Yalley-Ogunro J, Greenhouse J, Iraci N, Acosta EP, Barreca ML, Lewis MG, Savarino A. 2012. A highly intensified ART regimen induces long-term viral suppression and restriction of the viral reservoir in a simian AIDS model. PLoS Pathog 8:e1002774. https://doi.org/10.1371/journal.ppat.1002774.
13. Cottrell ML, Yang KH, Prince HMA, Sykes C, White N, Malone S, Dellon ES, Madanick RD, Shaheen NJ, Hudgens MG, Wulff J, Patterson KB, Nelson JAE, Kashuba A. 2016. A translational pharmacology approach to predicting outcomes of preexposure prophylaxis against HIV in men and women using tenofovir disoproxil fumarate with or without emtricitabine. J Infect Dis 214:55–64. https://doi.org/10.1093/infdis/jiw077.
14. Anderson PL, Kiser JJ, Gardner EM, Rower JE, Meditz A, Grant RM. 2011. Pharmacological considerations for tenofovir and emtricitabine to prevent HIV infection. J Antimicrob Chemother 66:240–250. https://doi.org/10.1093/jac/dkq447.
15. Pantaleo G, Graziosi C, Butini L, Pizzo PA, Schnittman SM, Kotler DP, Fauci AS. 1991. Lymphoid organs function as major reservoirs for human immunodeficiency virus. Proc Natl Acad Sci U S A 88:9838–9842. https://doi.org/10.1073/pnas.88.21.9838.
16. Mattapallil JJ, Douek DC, Hill B, Nishimura Y, Martin M, Roederer M. 2005. Massive infection and loss of memory CD4+ T cells in multiple tissues during acute SIV infection. Nature 434:1093–1097. https://doi.org/10.1038/nature03501.
17. Lin JH. 1995. Species similarities and differences in pharmacokinetics. Drug Metab Dispos 23:1008–1021.
18. Lin JH. 1998. Applications and limitations of interspecies scaling and in vitro extrapolation in pharmacokinetics. Drug Metab Dispos 26:1202–1212.
19. Thompson CG, Bokhart MT, Sykes C, Adamson L, Fedoriw Y, Luciw PA, Muddiman DC, Kashuba ADM, Rosen EP. 2015. Mass spectrometry imaging reveals heterogeneous efavirenz distribution within putative HIV reservoirs. Antimicrob Agents Chemother 59:2944–2948. https://doi.org/10.1128/AAC.04952-14.
20. Mavigner M, Habib J, Deleage C, Rosen E, Mattingly C, Bricker K, Kashuba A, Amblard F, Schinazi RF, Jean S, Cohen J, McGary C, Paiardini M, Wood MP, Sodora DL, Silvestri G, Estes J, Chahroudi A. 2018. Simian immunodeficiency virus persistence in cellular and anatomic reservoirs in antiretroviral-suppressed infant rhesus macaques. J Virol 92:e00562-18. https://doi.org/10.1128/JVI.00562-18.
21. Thompson CG, Rosen EP, Prince HMA, White N, Sykes C, de la Cruz G, Mathews M, Deleage C, Estes JD, Charlins P, Mulder LR, Kovarova M, Adamson L, Arora S, Dellon ES, Peery AF, Shaheen NJ, Gay C, Muddiman DC, Akkina R, Garcia JV, Luciw P, Kashuba A. 2019. Heterogeneous antiretroviral drug distribution and HIV/SHIV detection in the gut of three species. Sci Transl Med 11:eaap8758. https://doi.org/10.1126/scitranslmed.aap8758.
22. Alam C, Whyte-Allman S-K, Omeragic A, Bendayan R. 2016. Role and modulation of drug transporters in HIV-1 therapy. Adv Drug Deliv Rev 103:121–143. https://doi.org/10.1016/j.addr.2016.05.001.
23. Testa B, Crivori P, Reist M, Carrupt P-A. 2000. The influence of lipophilicity on the pharmacokinetic behavior of drugs: concepts and examples. Perspect Drug Discov Des 19:179–211. https://doi.org/10.1023/A:1008741731244.